Chinese sunspot drawings and their digitization – (III) quasi-biennial oscillation of the hand-drawn sunspot records

Miao Wan[1], Shu-Guang Zeng[1], Sheng Zheng[1] and Gang-Hua Lin[2]

[1] College of Science, China Three Gorges University, Yichang 443002, China; *zengshuguang19@163.com*
[2] National Astronomical Observatories, Chinese Academy of Sciences, Beijing 100101, China

Abstract Quasi-biennial Oscillations (QBOs) of the Sun have a significant meaning as a benchmark of solar cycle, not only for understanding the dynamo action but also in terms of space weather prediction. In this paper, the hand-drawn sunspot images recorded from the Purple Mountain Observatory are used to investigate the solar QBOs and the Gnevyshev gap of the sunspot relative numbers (Rs) and group sunspot numbers (Rg) during the period 1954–2011. The main results are as follows: (1) both the Rs and Rg exhibit similar periods including the 22-year magnetic cycle, the 11-year Schwabe cycle, and the QBOs modes; (2) the reconstructed QBOs of both data sets exhibit coherent behavior and tend to have a high amplitude during the maximum phase of each solar cycle; (3) the Gnevyshev gap is produced by the superposition of the QBOs and the 11-year Schwabe cycle, and the Rs is better to study the variation of the Gnevyshev gap rather than the Rg.

Key words: Sun: activity — Sun: sunspot — Sun: quasi-biennial oscillation

1 INTRODUCTION

The cyclic behavior of solar magnetic structures of the Sun driven by the dynamo action is one of the most interesting and important phenomena in solar physics fields. A wide variety of quasi-periodic oscillations have already been found with different parameters of the Sun. According to the length, the period on the Sun is defined in the light of short-term, mid-term and long-term (e.g., Deng et al. 2012; Singh et al. 2019). For the short-term periodicity, the most well-known is the rotation cycle with a value of 27 days that is attributed to the solar rotation (Gilman 1974). For the long-term periodicity, the most prominent periodicities are the 11-year Schwabe cycle (Schwabe 1844) that is closely related to the emergence and evolution of magnetic field, and the 22-year magnetic cycle (Hale et al. 1919) if one considers the heliomagnetic field polarity.

Periodicities between the 27-day rotation cycle and the 11-year Schwabe cycle are called the mid-term periodicity (Bai 2003). Lots of authors have searched for the existence of the mid-term periodicity in various solar activity indices following the discoveries of a nearly two-year oscillation in the 10.7 cm radio flux from 1947 to 1964 (Belmont et al. 1966) and a 154-day periodicity obtained with the high-energy flares (Rieger et al. 1984). The nearly two-year

oscillation in solar activity indicators is the quasi-biennial oscillations (QBOs), which might be related to the internal structure of the solar magnetic field. (Rieger et al. 1984; Bai 2003). Many studies have shown that the solar QBOs occur in almost all indices that described the solar activities in the photosphere, chromosphere and corona. For example, Akioka et al. (1987) found a 17-month of period time in the number and area of sunspot groups. Richardson et al. (1994) reported on the 1.3 yr of period time in the solar wind speed data from 1987 to 1993. Wang & Sheeley (2003) also found periodicities in sunspot area on timescales from 0.2 to 2.6 yr. Badalyan & Obridko (2004) discovered the 1.3 yr periodicity in the correlation of the greenline intensity and magnetic field in the lower corona, while Vecchio & Carbone (2009) found that the QBOs in the green coronal line emission whose period varied with time within the scope of 1.5–4 yr. By using time-frequency analysis techniques, the solar QBOs are found to exist in the chromospheric Hα flare index (Deng et al. 2013), in the high-latitude solar activity representing as the polar faculae (Deng et al. 2014), and in the green-coronal emission intensity (Deng et al. 2015). Moreover, Vecchio et al. (2012) discovered that the QBOs in the galactic cosmic ray intensity and they demonstrated

that the QBOs are actually responsible for the Gnevyshev gap phenomenon.

However, there is no clear mechanism to fully explain the QBOs nature. Most of authors believe that the QBOs are intrinsic to the solar dynamo mechanism (Benevolenskaya 1998; Howe et al. 2000; Krivova & Solanki 2002; Mursula et al. 2003; Mursula & Vilppola 2004; Cadavid et al. 2005; Vecchio et al. 2012; Popova & Yukhina 2013). Benevolenskaya (1998) proposed two dynamos to explain the QBOs in the surface magnetic field, one is at the base of the convection zone and the other is near the bottom of the layer below the solar surface. Wang & Sheeley (2003) thought that the QBOs was determined by the decay timescale of the equatorial dipole. An optional interpretation is that the instability of magnetic Rossby waves led to the periodic magnetic flux emergence, and it could be the cause of the QBOs (Lou 2000; Knaack & Stenflo 2005; Zaqarashvili et al. 2010). Therefore, the question of the mechanism of the QBOs is broadly open. More importantly, the QBOs of the Sun have a significant meaning as a benchmark of solar cycle, not only for understanding the dynamo action but also in terms of space weather prediction.

The possible origin of the solar QBOs and the Gnevyshev gap might be related to the solar tachocline, where several dynamical processes take place. For example, the solar rotation variation and the angular momentum are close to the tachocline level. Furthermore, the spatial distribution, including the north-south asymmetry and phase asymmetry of the solar QBOs should be revealed by the historical sunspot data (Deng et al. 2019).

To get better knowledge on the solar cycle and its effects of the whole heliosphere, the recovery, digitization and analysis of the historical observations have begun in recent years. Lin et al. (2019) digitized and constructed the parameters based on the Chinese historical sunspots drawings from 1925 to 2015. However, statistical work has to be followed in order to obtain the hidden scientific information. In this paper, the synchrosqueezing wavelet transform (SWT) (Daubechies et al. 2011) is applied to investigate the solar QBOs and the Gnevyshev gap of the sunspot relative numbers (Rs) and group sunspot numbers (Rg) of the hand-drawn sunspot records from the Purple Mountain Observatory. The structure of this paper is as follows: the data source and the analysis method are introduced in the next Section. In Section 3, the experimental process and the analysis results are presented. Finally, the conclusion and discussion are given in Section 4 .

2 DATA SOURCE AND ANALYSIS METHOD

2.1 Data Source

The time interval of the hand-drawn sunspot records derived from the Purple Mountain Observatory is 55 years covering from March 1954 to December 2011. More than 20 000 hand-drawn sunspot images were recorded, including the number of sunspots and group sunspots. We use the hand-drawn sunspot records from Yunnan Astronomical Observatory to fill a two-year gap mostly during the years of 1983 and 1984. Figure 1 shows the monthly distribution of the Rs and Rg of the Purple Mountain Observatory from March 1954 to December 2011, in which the missing data in 1983 and 1984 are filled by the hand-drawn sunspot records from Yunnan Observatory.

2.2 Synchrosqueezing Wavelet Transform

The synchrosqueezing wavelet transform (SWT) is a time-frequency redistribution method, which combines the wavelet transform and the spectral rearrangement. This method is firstly proposed by Daubechies et al. (2011). It is based on the wavelet transform to squeeze and rearrange the wavelet coefficient spectrum in the scale direction by the size of each element module, and finally get the time-frequency spectrum with more concentrated energy on the time-frequency surface by mapping. Compared to the traditional time-frequency analysis method, the SWT improves the resolution of time-frequency analysis and can clearly display the frequency components in the time-frequency diagram. The steps of the SWT are as follows:

First, the algorithm performs continuous wavelet transform (CWT) on a signal $f(t)$, and the obtained wavelet coefficient is $W_f(a, b)$. The expression is:

$$W_f(a, b) = \frac{1}{\sqrt{a}} \int_{-\infty}^{+\infty} f(t) \psi^* \left(\frac{t - b}{a} \right) d\mathrm{t} \,, \quad (1)$$

where a is the scale factor, b is the time shift factor, ψ^* is a conjugate wavelet function. According to the Plancherel theorem, the equivalent transformation in the frequency domain is:

$$W_f(a, b) = \frac{1}{2\pi} \int \frac{1}{\sqrt{a}} \hat{f}(\xi) \hat{\varphi}^*(a\xi) e^{jb\xi} d\xi \,, \quad (2)$$

where ξ represents the frequency, $\hat{f}(\xi)$ and $\hat{\varphi}(\xi)$ are respectively expressed as the Fourier transforms of $f(t)$ and $\psi(t)$.

If $\hat{\varphi}(\xi)$ concentrates at $\xi = \omega_0$, then $W_f(a, b)$ will be concentrated at the scale of $a = \omega_0/\omega$. However, $W_f(a, b)$ tends to disperse in the time-scale surface of $a = \omega_0/\omega$. Daubechies et al. (2011) pointed out that $W_f(a, b)$ will be
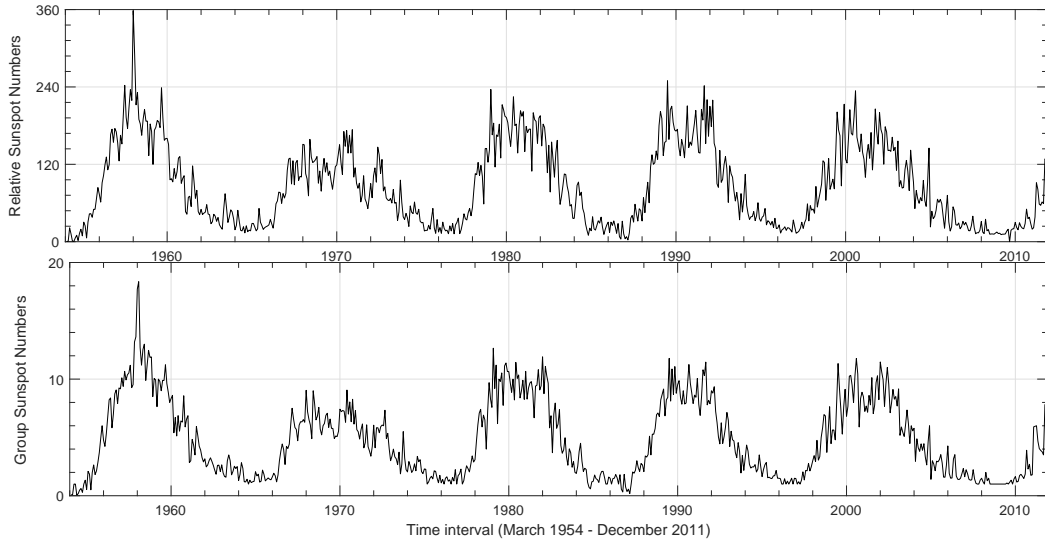
Fig. 1 Monthly distribution of the sunspot relative numbers (Rs) and group sunspot numbers (Rg) recorded from the Purple Mountain Observatory during the period of March 1954 – December 2011.

scattered in the scale direction, no matter what the value of scale a is, its oscillation characteristics in the time direction always point to the initial frequency ω. For any point (a, b), if the corresponding coefficient $W_f(a, b) \neq 0$, then the corresponding candidate frequency is:

$$w_s(a, b) = -i \left(W_f(a, b) \right)^{-1} \frac{\partial}{\partial b} W_f(a, b), \qquad (3)$$

where i represents an imaginary unit. According to this correspondence relation, the wavelet coefficients are differentiated and the instantaneous frequency is calculated, then the time-scale plane can be converted into the time-frequency plane. The specific method of synchronous extrusion is to squeeze the wavelet coefficients corresponding to the candidate frequencies in the interval $\left[\omega_l - \frac{1}{2}\Delta\omega, \omega_l + \frac{1}{2}\Delta\omega \right]$ near any frequency ω_1 to the center frequency ω_l. So, the synchrosqueezing wavelet transform is defined as:

$$T_s(\omega_l, b) = (\Delta\omega)^{-1} \sum_{a_k} : \left| \omega(a_k, b) - \omega_l \leq \frac{\Delta\omega}{2} \right|$$
$$W_f(a_k, b) \, a_k^{-3/2} (\Delta a)_k, \qquad (4)$$

where a_k represents the discrete scale, with a scale step $\Delta a = a_k - a_{k-1}$, $\Delta\omega = \omega_l - \omega_{l-1}$. The inverse transformation of the synchrosqueezing wavelet transform is defined as:

$$s(b) = \text{Re} \left[C_\psi^{-1} \sum_l T_s(\omega_l, b) (\Delta\omega) \right], \qquad (5)$$

where $C_\psi = \frac{1}{2} \int_0^\infty \psi(\xi) \xi^{-1} d\xi$, is a normalization constant from the selected wavelet and Re denotes the real part of the discrete SWT. A more detailed treatment

process can be found in Daubechies et al. (2011) and Thakur et al. (2013).

Feng et al. (2017) is the first paper that applied the SWT technique to study solar physics data. In their work, the SWT was used to investigate the midterm periodic variations of the Magnetic Plage Strength Index (MPSI) and the Mount Wilson Sunspot Index (MWSI) between 1970 January 19 and 2012 January 22. Short, mid and longer-term periodicities were represented and decomposed by the SWT with hardly any mode mixing. Recently, Deng et al. (2020a) applied the SWT technique to extract the main components of the polar faculae (high-latitude solar activity) in the northern and southern hemispheres for the time interval from 1951 August to 1998 December. Following their work, we apply the SWT method to analyze the sunspot number in this paper. Here, the bump wavelet is chosen, and the bin value is set to 4.

3 ANALYSIS RESULTS

By applying the SWT technique, the frequency content of the Rs and Rg, respectively, are displayed in Figures 2 and 3. To better describe the local components existing in the time-frequency pattern, the period scales in the two ranges of 0.5–2.0 years and 4–20 years are shown in the upper and lower panels in each figure. From these two figures, one can easily see that their frequency spectra contain many complex components, with the highest concentration of energy around the 11-year Schwabe cycle. That is, both the Rs and Rg have the characteristics around the 11-year Schwabe cycle. From the lower panels in both Figures 2 and 3, low frequency components also exist on timescales from 4 to 20 years, except for the 11-year Schwabe cycle. From the upper panels in these two figures, they exist
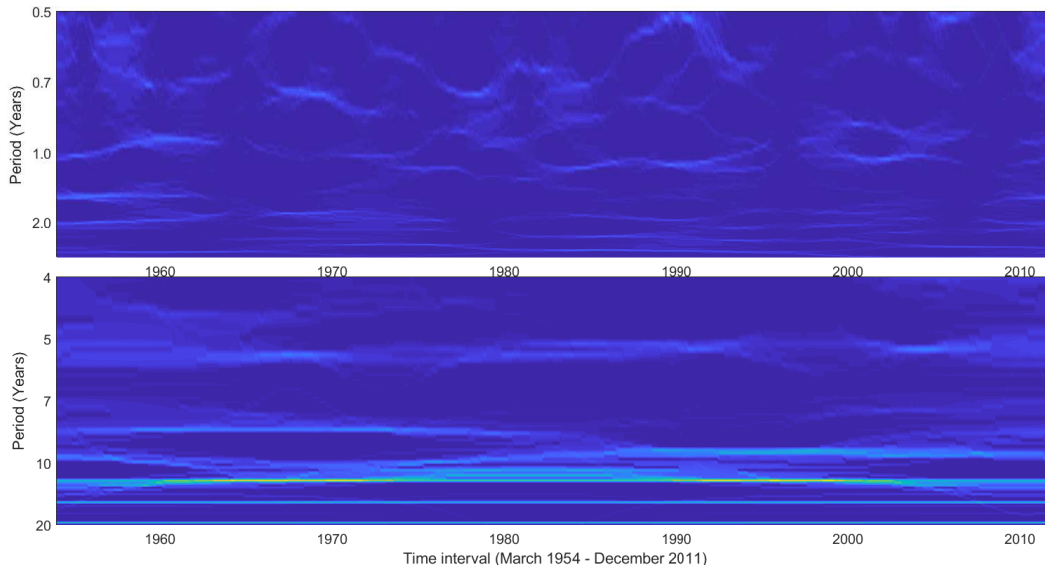
Fig. 2 The frequency spectra of the Rs by applying the SWT technique, with the period scales in the 0.5–2.0 years (*upper panel*) and 4–20 years (*lower panel*), respectively.
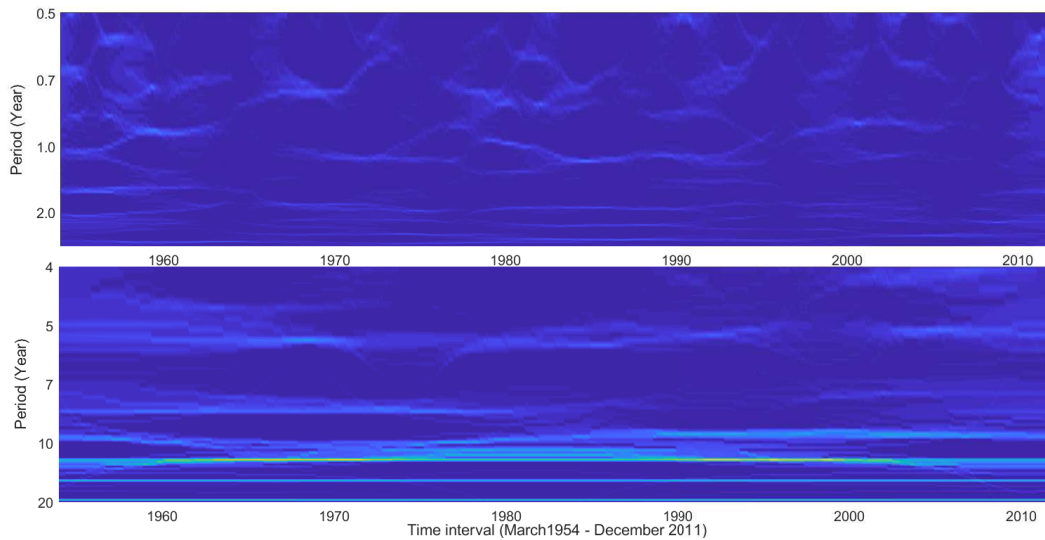

Fig. 3 The frequency spectra of the Rg by applying the SWT technique, with the period scales in the 0.5–2.0 years (*upper panel*) and 4–20 years (*lower panel*), respectively.

many high frequency components in the ranges of 0.5–2.0 years, especially the QBOs which shows very clearly and smoothly.

In order to explore the cyclic behaviors of the Rs and Rg in detail, eight period modes are decomposed in each of the two data sets, and are shown in Figures 4 and 5, respectively. We calculate the typical values of eight periodic modes and list them in Table 1. As Table 1 reported, one can see that the longest mode (IM1) is around 21 year periodicity, which is the so-called 22-year Hale cycle (magnetic cycle). The 22-year Hale magnetic cycle is first found by Hale & Nicholson (1925) whose study focused on the magnetic polarities of sunspot groups observed on Mount Wilson between 1908 and 1925.

The best-known 11-year Schwabe cycle (IM2) is clearly revealed. For the shortest mode (IM8), the periodicity is 0.17 years, which is related to the time interval of the data sets. We use the mean monthly number of the Rs and Rg of the Purple Mountain Observatory, the time interval of the data sets is one month. According to the Nyquist's sampling law, the sampling frequency must be greater than or equal to twice of the highest frequency in the signal so that the information in the original signal can be retained completely.

For the modes 3 and 4, the timescales around 7.7 years and 5.3 years can be interpreted as the third and fourth harmonic of the 22-year magnetic cycle. For example, using the modified coronal index for the time interval from
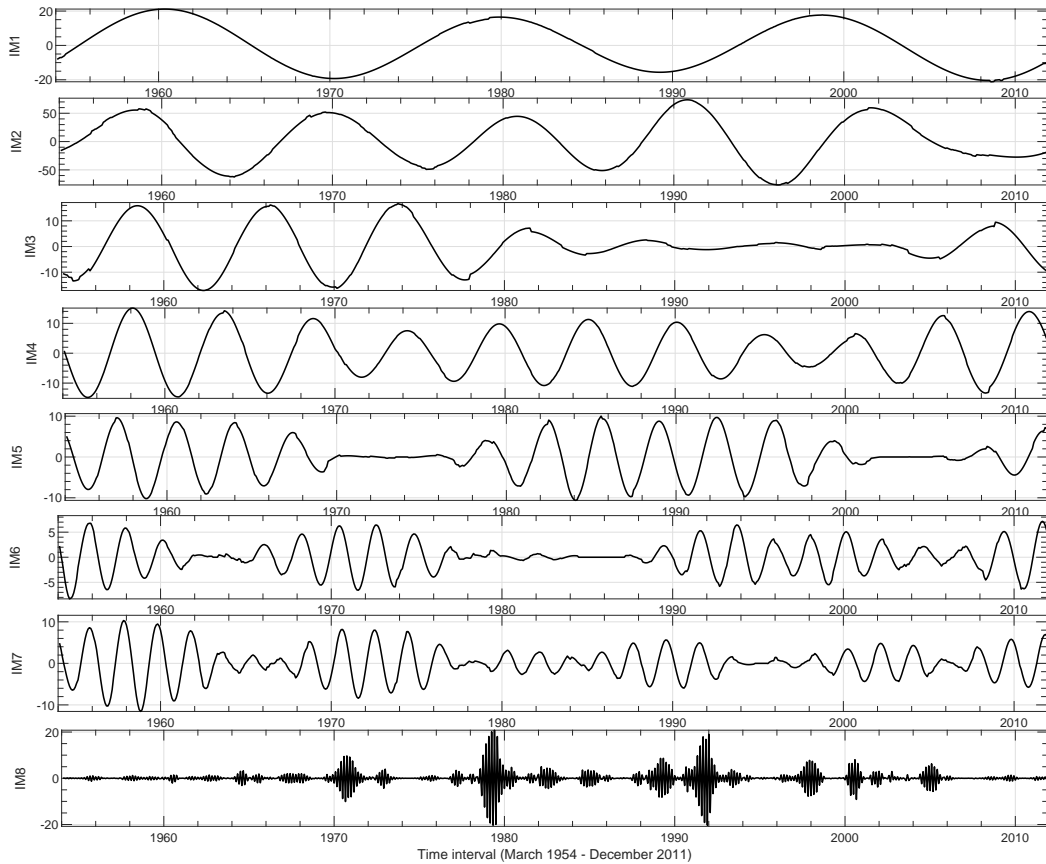
Fig. 4 The periodic modes of the Rs decomposed and reconstructed by using the SWT technique.

1939 January 1 – 2019 May 31, Deng et al. (2020b) studied the systematic regularities of solar coronal rotation, and found that a periodicity of around 6 years existing in the period length of coronal rotation, and was considered as a close relationship with the 22-year Hale cycle. Further studies are needed to reveal the physical origin of the periodicity around 5–7 years.

Beyond that, according to the definition of the solar QBOs (in the range between 0.5–4 years), the periodicity of 3.45 year (IM5), 2.18 year (IM6), and 1.94 year (IM7) in the Rs, and those of 3.36 year (IM5), and 1.88 year (IM6)in the Rg are taken as a part of the QBOs modes. To reconstruct the solar QBOs in each of the two data sets, the periodic modes from 5 to 7 are summed.

To better understand the relationship between the 11-year Schwabe cycle and the solar QBOs, we extracted and superimposed them, which were shown in Figure 6. It is worthwhile to notice that the amplitudes of the solar QBOs in the Rs and Rg exhibit intermittent behaviors, and are modulated by the 11-year solar cycle. That is, the solar QBOs tend to have a high amplitude during the maximum phases of each solar cycle. More interestingly, our analysis on the 11-year Schwabe cycle and the QBOs modes shows a new feature, the so-called Gnevyshev gap, exhibiting two

activity waves, the first one with the maximum at the end of the rising phase and the second one at the start of the declining phase of a solar cycle (Gnevyshev 1967). From the bottom panel of Figure 6, we demonstrate that the superposition of the solar QBOs and the 11-year Schwabe cycle produces the Gnevyshev gap, in other words, the Gnevyshev gap is actually a consequence of the QBOs modulated by the 11-year Schwabe cycle. Furthermore, we found that the Rs is better to study the Gnevyshev gap rather than the Rg. In the last decade, Benevolenskaya (1998) firstly argued that one of the typical features of the solar QBOs is a temporal weakening of solar indices observed in the maximum time of a solar cycle. That is, the solar QBOs and the Gnevyshev gap have a close relationship. Our analysis results confirm their conclusion.

4 CONCLUSIONS AND DISCUSSION

Based on the data sets of the Rs and Rg derived from the hand-drawn sunspot records from the Purple Mountain Observatory during the period of March 1954 to December 2011, the SWT technique is applied to decompose these two data sets and we have obtained eight periodicity modes. The 11-year Schwabe cycle and the QBOs modes of both data sets were well extracted and reconstructed. To
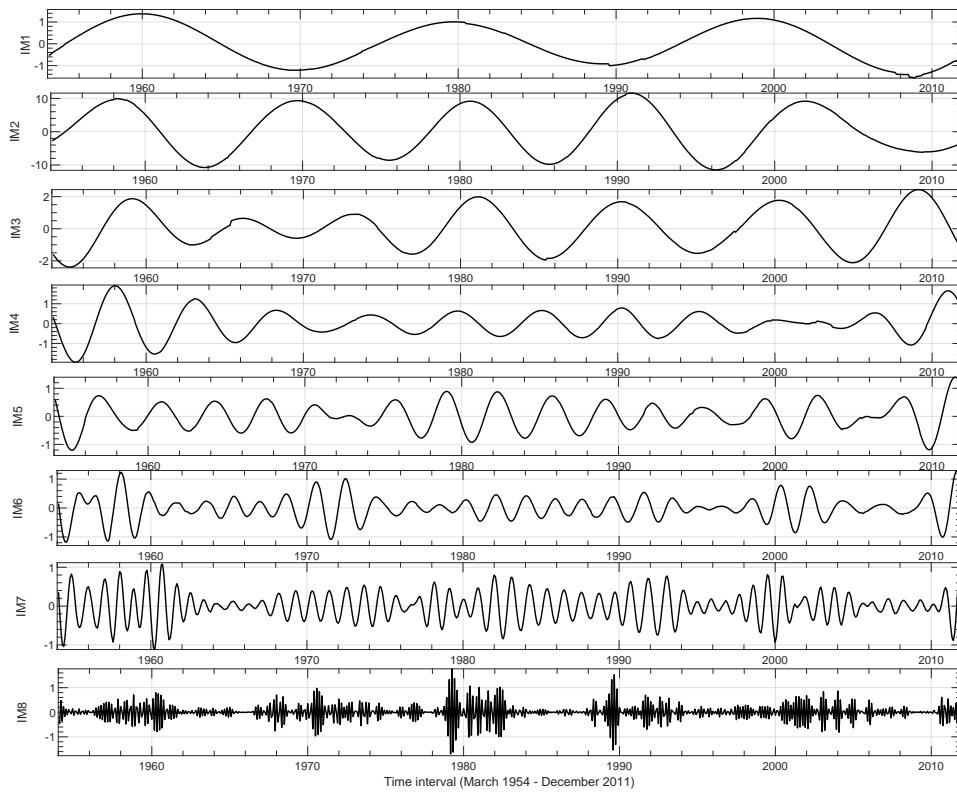
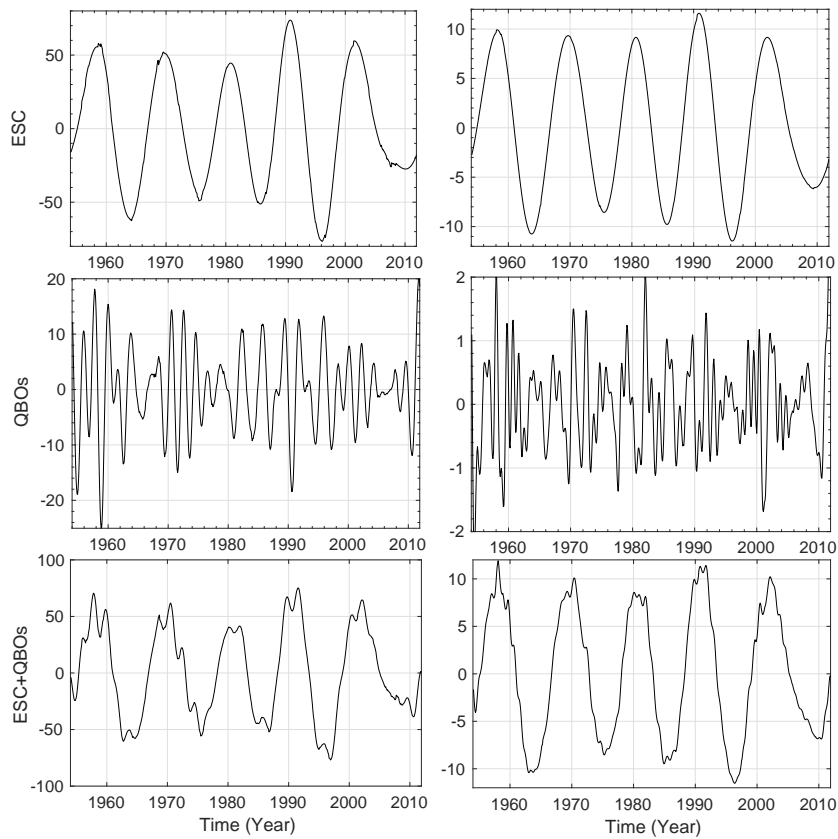**Fig. 5** The periodic modes of the Rg decomposed and reconstructed by using the SWT technique.

Fig. 6 *Top panels*: the 11-year Schwabe cycle periodicity of the Rs and Rg. *Middle panels*: the QBOs modes of the Rs and Rg. *Bottom panels*: the superposition of the QBOs modes and the 11-year Schwabe cycle of the Rs and Rg.

Table 1 Periodic Values in Each of the Eight Modes in the Rs and Rg

Mode	Period (yr)	
	Rs	Rg
1	21.02	21.14
2	10.55	10.65
3	7.70	7.92
4	5.33	5.32
5	3.45	3.36
6	2.18	1.88
7	1.94	1.08
8	0.17	0.17

better study the relationship between the 11-year Schwabe cycle and the QBOs modes, we superimposed them to show the interesting structure called the Gnevyshev gap. Our main results are as follows.

(1) By using the SWT method, the frequency content of the Rs and Rg are clearly decomposed. Both of these two data sets have similar periods including the 22-year Hale cycle, the 11-year Schwabe cycle and the QBOs modes.

(2) By superimposing the 11-year Schwabe cycle and the QBOs modes, the Gnevyshev gap is reproduced unexpectedly. We confirm that the Gnevyshev gap is actually a consequence of the QBOs modulated by the 11-year Schwabe cycle. Through careful analysis, we find that the Rs is better to study the Gnevyshev gap rather than the Rg.

The solar QBOs cannot be obtained without a preparatory filtration, and we have seen that different time-frequency analysis methods by many authors have show their capabilities to verify its existence. Compared to the empirical mode decomposition method, the SWT has a strict mathematical derivation process that supports reconstruction of the time-frequency map to obtain the time-domain components of each frequency component. Our analysis results show that the SWT technique for the periodic analysis of the hand-drawn sunspot records is very effective.

References

Akioka, M., Kubota, J., Suzuki, M., et al. 1987, Solar physics, 112, 313

Badalyan, O. G., & Obridko, V. N. 2004, Astronomy Reports, 48, 678

Bai, T. 2003, ApJ, 591, 406

Belmont, A. D., Dartt, D. G., & Ulstad, M. S. 1966, Journal of the Atmospheric Sciences, 23, 314

Benevolenskaya, E. E. 1998, ApJL, 509, L49

Cadavid, Lawrence, J. K., McDonald, D. P., & Ruzmaikin, A. 2005, Sol. Phys., 226, 359

Daubechies, I., Lu, J. f., & Wu, H. T. 2011, Applied and computational harmonic analysis, 30, 243

Deng, L. H., Fei, Y., Deng, H., Mei, Y., & Wang, F. 2020a, MNRAS, 494, 4930

Deng, L. H., Gai, N., Tang, Y. K., Xu, C. L., & Huang, W. J. 2013, Ap&SS, 343, 27

Deng, L. H., Li, B., Xiang, Y. Y., & Dun, G. T. 2014, Advances in Space Research, 54, 125

Deng, L. H., Li, B., Xiang, Y. Y., & Dun, G. T. 2015, Journal of Atmospheric and Solar-Terrestrial Physics, 122, 18

Deng, L. H., Qu, Z. Q., Wang, K. R., & Li, X. B. 2012, Advances in Space Research, 50, 1425

Deng, L. H., Zhang, X. J., Deng, H., Mei, Y., & Wang, F. 2020b, MNRAS, 491, 848

Deng, L. H., Zhang, X. J., Li, G. Y., Deng, H., & Wang, F. 2019, MNRAS, 488, 111

Feng, S., Yu, L., Wang, F., et al. 2017, ApJ, 845, 11

Gilman, P. A. 1974, ARA&A, 12, 47

Gnevyshev, M. N. 1967, Sol. Phys., 1, 107

Hale, G. E., Ellerman, F., Nicholson, S. B., & Joy, A. H. 1919, ApJ, 49, 153

Hale, G. E., & Nicholson, S. B. 1925, ApJ, 62, 270

Howe, R., Christensen-Dalsgaard, J., Hill, F., et al. 2000, Sci., 287, 2456

Knaack, R., & Stenflo, J. O. 2005, A&A, 438, 349

Krivova, N. A., & Solanki, S. K. 2002, A&A, 394, 701

Lin, G. H., Wang, X. F., Liu, S., et al. 2019, Sol. Phys., 294, 79

Lou, Y. Q. 2000, ApJ, 540, 1102

Mursula, K., & Vilppola, J. H. 2004, Sol. Phys., 221, 337

Mursula, K., Zieger, B., & Vilppola, J. H. 2003, Sol. Phys., 212, 201

Popova, E. P., & Yukhina, N. A. 2013, Astronomy Letters, 39, 729

Richardson, J. D., Paularena, K. I., Belcher, J. W., & Lazarus, A. J. 1994, Geophysical Research Letters, 21, 1559

Rieger, E., Share, G. H., Forrest, D. J., et al. 1984, Nature, 312, 623

Schwabe, H. 1844, Astronomische Nachrichten, 21, 233

Singh, P. R., Tiwari, C. M., Saxena, A. K., Agrawal, S. L., & Mishra, A. P. 2019, Ap&SS, 364, 59

Thakur, G., Brevdo, E., Fučkar, N. S., & Wu, H. T. 2013, Signal Processing, 93, 1079

Vecchio, A., & Carbone, V. 2009, A&A, 502, 981

Vecchio, A., Laurenza, M., Storini, M., & Carbone, V. 2012, Advances in Astronomy, 2012, 834247

Wang, Y. M., & Sheeley, N. R. 2003, ApJ, 590, 1111

Zaqarashvili, T. V., Carbonell, M., Oliver, R., et al. 2010, ApJL, 724, L95